10594 *J. Phys. Chem. A* **2004,** *108,* 10594−10601

Jahn−Teller Effect versus Spin−Orbit Coupling in X^2E CH_3S: An ab Initio Study by the Equation-of-Motion Coupled Cluster Method and Multiconfiguration Quasi-Degenerate Second-Order Perturbation Theory

Aleksandr V. Marenich and James E. Boggs*

Institute for Theoretical Chemistry, Department of Chemistry and Biochemistry,
The University of Texas at Austin, Austin, Texas 78712

Received: June 22, 2004

The equation-of-motion coupled cluster method (EOMIP) using a reference Slater determinant based on the CH_3S^--anion ground state with basis sets of triple- and quadruple-ζ quality was applied for numerical optimizations of geometries of stationary points on adiabatic Jahn−Teller surfaces of the X^2E ground state of CH_3S crossing at the C_{3v} symmetry nuclear configuration. Calculations by the multireference configuration interaction method and multiconfiguration quasi-degenerate second-order perturbation (PT2) theory were also performed with use of a complete active space CASSCF reference wave function. The linear and quadratic Jahn−Teller constants were computed for each of three Jahn−Teller active modes. The potential surfaces corresponding to spin−orbit states $^2E_{3/2}$ and $^2E_{1/2}$ were obtained with eigenenergies of the full Breit−Pauli spin−orbit operator with a PT2−CASSCF reference wave function. The one- and two-electron scalar relativistic effects were included in CASSCF and spin−orbit calculations. The calculated Jahn−Teller stabilization energy, the barrier to pseudorotation, and the spin−orbit splitting are 93, 15, and 358 cm^{-1}, respectively. The Jahn−Teller distortions are totally quenched by the strong spin−orbit coupling. The recommended values of the geometry parameters of CH_3S are $R_e(CS) = 1.794$ Å, $R_e(CH) = 1.087$ Å, and $\alpha_e(HCS) = 109.8°$.

Introduction

The methoxy radical (CH_3O) and its sulfur analogue (CH_3S) are important intermediates in atmospheric and combustion chemistry. Numerous references to the practical importance of CH_3O in astronomic, atmospheric, and combustion studies have been compiled.[1] According to ref 2, the methylthio radical (CH_3S) plays a significant role in the oxidation of products of natural sulfur emission in such forms as dimethyl sulfide (CH_3SCH_3), methanethiol (CH_3SH), and dimethyl disulfide (CH_3SSCH_3).

Both CH_3S and CH_3O are open-shell radical systems. They may demonstrate such effects as Jahn−Teller and spin−orbit couplings, which make a significant impact on all spectroscopic and structural properties of the radicals. The spin-vibronic interactions can lead to the well-known fact[3] that Jahn−Teller distortions can quench the electronic angular momentum and reduce the spin−orbit splitting and, vice versa, the spin−orbit coupling can quench the Jahn−Teller stabilization energy. Obviously, the spin-vibronic effects are able to bring complications into prediction of thermochemistry and kinetics of gas-phase processes involving these compounds.

The methoxy radical has been widely studied by laser-induced fluorescence, stimulated emission pumping, and photoelectron (photodetachment) spectroscopy (see refs 4 and 5). Numerous manifestations of Jahn−Teller coupling in the X^2E state of CH_3O were observed. A recent high level theoretical study[4] of the Jahn−Teller effect in X^2E CH_3O yields a moderate Jahn−Teller stabilization energy of 209 cm^{-1} that is much larger than the value of spin−orbit splitting (61.8 ± 0.6 cm^{-1}) predicted from the experiment.[1]

The CH_3S radical has been studied during the last three decades, though less extensively than the oxide. Spectroscopic studies of CH_3S were performed using emission,[6] microwave spectroscopy,[7] laser-induced fluorescence,[2,8,9] ultraviolet absorption spectroscopy,[10] electron photodetachment[11−13] of the thiomethoxyl (CH_3S^-) anion, and photodissociation spectroscopy of CH_3S[14,15] (see also references therein). Experimental results mostly demonstrate a relatively large spin−orbit splitting of the ground electronic state, in excess of 200 cm^{-1}, and the Jahn−Teller distortions are supposed to vanish.[3,9] The rotational transitions in the microwave spectrum[7] of CH_3S were observed to be split into doublets. The estimate of $R(C-S) = 1.791$ Å was obtained from the observed B rotational constant with fixed values of $R(C-H) = 1.090$ Å and $\angle HCS = 110°$.[7] The symmetric top rotational constant A of CH_3S was not explicitly obtained from this experiment.[7]

Suzuki et al. reported results of investigations of the CH_3S and CD_3S $A^2A_1-X^2E$ systems by laser-induced fluorescence.[8] They observed two progressions in the fluorescence excitation spectrum of CH_3S that were assigned to the transitions from the spin−orbit splitting levels ($^2E_{3/2}$ and $^2E_{1/2}$) to different C−S stretching (ν_3) vibrational levels of the $^2A_1$ state. To explain the difference of band shapes of the $^2A_1-^2E_{1/2}$ and $^2A_1-^2E_{3/2}$ transitions, the authors of ref 8 supposed that geometries of these spin−orbit sublevels are significantly different. The band shapes of doublets in the dispersed fluorescence spectrum of CH_3S are mostly similar to those of the excitation spectrum.[8] Only two fundamental vibrational frequencies of the CH_3S X^2E ground state were determined from the dispersed spectrum,[8] $\nu_2(A_1) = 1316 \pm 4$ and $\nu_3(A_1) = 740 \pm 4$ cm^{-1}. On the basis of rotational analysis of the $A^2A_1-X^2E$ laser-induced fluorescence spectrum of jet-cooled CH_3S,[9] Hsu, Liu, and Miller rejected the suggestion

---

* To whom correspondence should be addressed. E-mail: james.boggs@mail.utexas.edu. Fax: (512) 471-8696.

10.1021/jp040443f CCC: $27.50

of Suzuki et al.[8] about the difference of $^2E_{1/2}$ and $^2E_{3/2}$ geometries and showed that nearly all of the previously reported molecular parameters of CH_3S should be revised. They determined two rotational constants (A and B) in the CH_3S radical as a prolate symmetric top and two additional parameters h_1 and h_2 to characterize Jahn−Teller interactions in CH_3S. The X^2E ground-state geometry parameters, $R(C-S) = 1.767 \pm 0.012$ Å and $\angle HCH = 102.5 \pm 2.6°$, were evaluated at the fixed value of $R(C-H) = 1.10 \pm 0.02$ Å.[9] Another $A^2A_1-X^2E$ laser-induced fluorescence study of CH_3S was performed by Chiang and Lee.[2] They observed the main ($^2A_1-^2E_{3/2}$) and weak ($^2A_1-^2E_{1/2}$) progressions in the excitation spectrum of jet-cooled CH_3S, which were similar to those observed by Suzuki et al.[8] at room temperature except for a few new bands. The main progressions gave the following X^2E ground-state fundamentals (cm^{-1}): $\nu_2(A_1) = 1313 \pm 5$, $\nu_3(A_1) = 727 \pm 3$, and $\nu_5(E) = 1496 \pm 6$.[2] The evaluations of $\nu_1(A_1) = 2776$, $\nu_4(E) = 2706$, and $\nu_6(E) = 586$ cm^{-1} were less accurate because the relevant observed lines were weak and a limited number of them were identified. The values of ν_2 and ν_3 obtained by Suzuki et al.[8] in a static gas cell at room temperature are close to those observed by Chiang and Lee[2] in the jet-cooled CH_3S spectra. However, the latter approach is more accurate and gives more information about the vibrational structure of the dispersed fluorescence spectrum due to less band congestion at low temperatures.[2,3]

The technique of laser photoelectron spectrometry of negative ions based on detection of photodetached electrons provides electron affinities and some vibrational frequencies for both an anion and the resulting neutral molecule.[11] Only the totally symmetric fundamentals of CH_3S (ν_1 and ν_3) were measured in a recent study of the CH_3S^- anion by Schwartz et al.[13] The value of $\nu_3(A_1) = 725 \pm 15$ cm^{-1} (ref 13) reproduces very well $\nu_3(A_1) = 727 \pm 3$ cm^{-1} from the CH_3S dispersed fluorescence spectrum.[2] However, the $\nu_1(A_1)$ values (2960 ± 30[13] and 2776[2] cm^{-1}) are in significant disagreement. Other electron photodetachment experiments performed prior to the work of Schwartz et al.[13] gave the following values (in cm^{-1}): $\nu_2(A_1) = 1040 \pm 80$ and $\nu_3(A_1) = 680 \pm 40$ (ref 11); $\nu_2(A_1) = 1360 \pm 70$ and $\nu_3(A_1) = 770 \pm 50$ (ref 12). The CH_3-deformation fundamental $\nu_2(A_1)$ measured for CH_3S in ref 11 is too low in comparison with $\nu_2(A_1) = 1325 \pm 30$ cm^{-1} observed for CH_3O in the same photodetachment study and strongly contradicts the results of other spectroscopic investigations of CH_3S (see refs 2, 8, and 12).

Generally the experimental values ($-a\zeta_e d$) of spin−orbit splitting in CH_3S are in good agreement among themselves (in cm^{-1}): 220.3[7] (microwave spectroscopy); 259.1,[2] 280 ± 20,[8] and 255.5[9] (laser-induced fluorescence); 280 ± 50[12] and 265 ± 15[13] (photoelectron spectroscopy). The value from the microwave study[7] is less accurate because it was not measured directly. We should mention here that the observed values of spin−orbit splitting ($-a\zeta_e d$) are always an energy difference between two spin-vibronic levels each of which is approximately the product of the vibrational ground state and one of the two spin−orbit states ($^2E_{3/2}$ and $^2E_{1/2}$). In this case, the observed values of $a\zeta_e d$ may vary for different isotopic species (see for instance ref 8, -280 ± 20 cm^{-1} in CH_3S and -260 ± 20 cm^{-1} in CD_3S) unlike the value of $a\zeta_e$ that shows the spin−orbit splitting without Jahn−Teller coupling. The Ham reduction factor d ($d \leq 1$) shows how much the spin−orbit coupling is reduced by the Jahn−Teller effect. Using the spectroscopic data for CH_3S and CD_3S, Bent[18] calculated the coefficients d in CH_3S and CD_3S and evaluated the Jahn−Teller stabilization energy ($E_{JT} = 88-152$ cm^{-1} with the most likely value of 95 cm^{-1}) and the spin−orbit coupling in CH_3S ($-a\zeta_e = 327-377$ cm^{-1} with the most likely value of 356 cm^{-1}). However, these parameters should be reviewed because of the large uncertainties and the fact that Bent supposed $\nu_5(E)$ to be the only Jahn−Teller active mode in CH_3S. Supposing that another vibrational mode $\nu_6(E)$ is the only one responsible for the Jahn−Teller effect in CH_3S and using the ab initio values of the harmonic frequencies of CH_3S, Barckholtz and Miller[3] obtained somewhat different values of $E_{JT} = 41$ and $-a\zeta_e = 341$ cm^{-1}.

Analysis of the results of spectroscopic studies (see refs 2, 7−9, 11−13, and references therein) on the thiomethoxyl radical CH_3S forces us to conclude that experiments have not provided complete and totally reliable data about the structure and transition frequencies of CH_3S, especially for the fundamentals $\nu_1(A_1)$, $\nu_4(E)$, $\nu_6(E)$, and relevant overtones. Although the study by Chiang and Lee[2] has provided the most accurate experimental results presently, the experimental accuracy is not enough to identify those weak lines in the dispersed fluorescence spectrum of jet-cooled CH_3S, which may be assigned to vibrations along Jahn−Teller active modes. According to ref 3, Jahn−Teller coupling in CH_3S is small, otherwise greater intensities would be detected for lines associated with the Jahn−Teller active modes.

Numerous references to results of theoretical studies of CH_3O are given in ref 4. There are also a few calculations of the heavier CH_3S radical (see for instance refs 13, 16, and 17). Barckholtz and Miller[16] made the first attempt at quantitative ab initio predictions of the spectroscopic parameters to characterize the Jahn−Teller potential surfaces of the CX_3Y methoxy family radical (CH_3O, CH_3S, CF_3O, and CF_3S). The 6-31G* basis sets and the state-averaged complete active space self-consistence field (CASSCF) method were applied.[16] Quadratic Jahn−Teller constants were obtained from restricted open-shell Hartree−Fock (ROHF) calculations.[16] Optimization of geometries at specific points on the adiabatic potential surfaces of CX_3Y was followed by calculations of harmonic frequencies.[16] Höper, Botschwina, and Köppel[4] performed a variational calculation of vibronic energies for the methoxy radical. All the linear, quadratic, and bilinear coupling vibronic constants of CH_3O were calculated by the multireference configuration interaction method with a CASSCF reference.[4] Analysis of results of previous theoretical studies of CX_3Y shows that the most rigorous ab initio approach should include dynamical electron correlation (for instance by the multireference configuration interaction method) and the spin−orbit coupling. The latter has never been taken into account for CX_3Y by means of ab initio methods. The role of spin−orbit and other relativistic effects may be very significant for the electron and nuclear dynamics in the heavier species such as CH_3S and CF_3S.

The present theoretical study is intended to provide a more accurate ab initio evaluation of the molecular parameters of CH_3S as well as to review experimental data on the basis of our evaluations. We report here results of our first investigations of vibronic and spin−orbit interactions in CH_3S performed at a high level of theory using basis sets of triple- and quadruple-ζ quality and multiconfigurational methods to account for dynamic electron correlation. The equation-of-motion coupled cluster method (EOM-CCSD), the multiconfiguration quasi-degenerate second-order perturbation theory (PT2), and the multireference configuration interaction approach with all doubles and singles (SOCI) were applied in calculations of Jahn−Teller parameters of CH_3S. The spin−orbit correction to the total energy of CH_3S was calculated. The secondary purpose of the work is to make comparison of the computational accuracy of different approaches which may be applied in studies of the CX_3Y vibronic systems.

Details of Computations

Solution of the Electron Problem. We performed computations by EOMIP with use of a local version of the ACES II program package[19] and by CASSCF, PT2, and SOCI with the GAMESS (US) package.[20] We used the correlation consistent polarized valence basis sets of Dunning et al.[21] of triple- and quadruple-ζ quality (further abbreviated to pvtz and pvqz, respectively). The linear combinations of symmetry-adapted basis functions were created only by means of pure spherical harmonics in all the computations of CH_3S. The total number of basis functions included in the MO variation spaces was 106 (pvtz) and 204 (pvqz). The two core molecular orbitals [1s (C, S)] were dropped in coupled cluster and perturbation theory calculations of CH_3S.

We used the equation-of-motion coupled cluster method with a reference Slater determinant $|0\rangle$ based on the CH_3S^--anion ground state (further abbreviated to EOMIP).[22] The main idea of EOMIP theory is the description of final (neutral) states by means of the diagonal representation of the similarity transformed electron Hamiltonian in a basis comprised of all determinants obtained from $|0\rangle$ by removing a single electron and those determinants that also involve promotion of another electron to an orbital that is not occupied in $|0\rangle$.[22] The accuracy of EOMIP was shown to be comparable to that obtained in relatively large scale and much more time expensive multireference configuration interaction calculations of doublet radicals.[22] The T_n amplitudes of the CCSD wave function obtained for X^1A_1 CH_3S^- were of small magnitude lying under 0.011 (T_1) and 0.054 (T_2).

As an alternative, we performed energy calculations by the multiconfiguration quasi-degenerate second-order perturbation theory (PT2) and the multireference (second order) configuration interaction approach with all doubles and singles (SOCI).[20] In both cases, we used a CASSCF reference wave function, the molecular orbitals being optimized with equal weights for both E states. Analysis of the CH_3S electronic structure allowed us to separate six molecular orbitals $[(a_1)^2(a_1)^2(a_1)^2(a_1)^2(e)^4]$ assigned approximately to atomic basis functions 1s (C) and 1s, 2s, 2p (S) and seven valence ones $[(a_1)^2(a_1)^2(e)^4(a_1)^2(e)^3]$. The smallest active space $(a_1)^2(e)^3(a_1)^0$ in our calculations included five electrons in four orbitals, where the e orbitals could be interpreted as the S 3pπ lone pairs and the a_1 orbitals as the C−S σ and σ* MOs. The larger complete active spaces (13 electrons in 8 orbitals [$4a_1 + 2e$] and 13 electrons in 11 orbitals [$5a_1 + 3e$]) were studied only at the pvtz basis set level. The total number of configuration state functions (CSFs) in these CASSCF calculations was 20, 168, and 76 230, respectively. The initial molecular orbital set for the smallest CAS was obtained from the restricted Hartree–Fock calculation for CH_3S^-. The starting molecular orbitals for more extensive CASSCF calculations were taken from computations with a smaller CAS. This approach gave good convergence for the CAS optimization routine. The doubly occupied molecular orbitals were optimized.

The complete active space including 13 electrons in 8 orbitals was used in our SOCI calculations, as many as 13 940 178 single and double configurations being generated by the promotion of one or two electrons from the active space orbitals to all virtual ones. We used the PC GAMESS version[23] of the GAMESS (US) program[20] with the implemented graphical unitary group approach (GUGA) CI Hamiltonian packing to save disk space. The formalism of multiconfiguration quasi-degenerate second-order perturbation theory was described by Nakano.[24] All the molecular orbitals (doubly occupied, active space, and virtual MOs) were correlated in perturbation calculations with the exception of two core molecular orbitals 1s (C, S).

The PT2 computations were followed by evaluation of spin−orbit coupling (SOC) as a second-order perturbative correction to the PT2 total energy (SOCPT2) with use of GAMESS.[20] The reference CAS in SOCPT2 calculations consisted of five electrons in four orbitals ($2a_1 + e$). The final spin-mixed states ($^2E_{3/2}$ and $^2E_{1/2}$) were obtained by means of the full Breit−Pauli spin−orbit operator composed of one- and two-electron components (see details in ref 25). Inclusion of the SOC treatment into multireference perturbation theory allows one to account for the dynamical electron correlation in SOC calculations.

The one- and two-electron spin-independent relativistic effects were involved in CASSCF, PT2, and SOCPT2 calculations by means of the elimination of the small components of relativistic wave functions (the RESC scheme).[20,25,26]

Calculations of Vibronic Constants. As predicted by the Jahn−Teller theorem, the C_{3v} symmetry nuclear configuration in the X^2E ground electronic states is expected to be unstable. There are two specific points on the adiabatic potential energy surface (PES) of CH_3S corresponding to distorted (C_s symmetry) nuclear configurations (a minimum and a saddle point) with electron wave functions of A′ or A″ symmetries.[4,16]

Optimizations of geometry parameters and calculations of harmonic frequencies for C_{3v}(E), C_s(A′), and C_s(A″) nuclear configurations were performed numerically using the symmetry coordinates (S) and the program ANOCOR.[27] The set of coordinates used for the C_{3v} symmetry structure of CH_3S is shown on Figure 1. The vector **S** is related to the vector of normal coordinates (**Q**) by means of the matrix **L** that can be obtained by the GF method[28]

$$\mathbf{S} = \mathbf{L}\,\mathbf{Q} \tag{1}$$

The unperturbed harmonic frequencies ω_4(E), ω_5(E), and ω_6(E) were calculated by numerical differentiation of average energies U_0 expressed through total energies (U_+ and U_-) of the two electronic states crossing at the C_{3v} symmetry point[16]

$$U_0 = {}^1/_2(U_+ + U_-) \tag{2}$$

The average potential U_0 is relevant to the hypothetical case when a Jahn−Teller perturbation totally vanishes. The Jahn−Teller stabilization energy (E_{JT}) is determined as $E_{JT} = U(C_{3v}, \mathrm{E}) - U(C_s, \mathrm{A}')$ where $U(C_{3v}, \mathrm{E})$ and $U(C_s, \mathrm{A}')$ are total energies corresponding to the C_{3v}(E) and C_s(A′) equilibrium geometries, respectively. The barrier to pseudorotation (Δ_{JT}), or the quadratic Jahn−Teller stabilization energy, is $\Delta_{JT} = U(C_s, \mathrm{A}'') - U(C_s, \mathrm{A}')$. The quantities of E_{JT} and Δ_{JT} calculated along the a component of any of the E-type normal coordinates (Q_{4a}, Q_{5a}, and Q_{6a}) are measures of a net Jahn−Teller effect for this vibrational mode. With use of the expressions from refs 3 and 16, we established the following relations between E_{JT}, Δ_{JT}, an unperturbed harmonic frequency ω, linear (k, D), and quadratic (K, g) vibronic constants

$$K = \Delta_{JT}/(2E_{JT} - \Delta_{JT}) \tag{3}$$

$$D = E_{JT}\,(1 - K)/\omega \tag{4}$$

$$g = \omega\,K \tag{5}$$

$$k = \pm[2E_{JT}\,\omega\,(1 - K)]^{1/2} \tag{6}$$

where the quantities E_{JT}, Δ_{JT}, ω, g, and k are expressed in cm^{-1}.

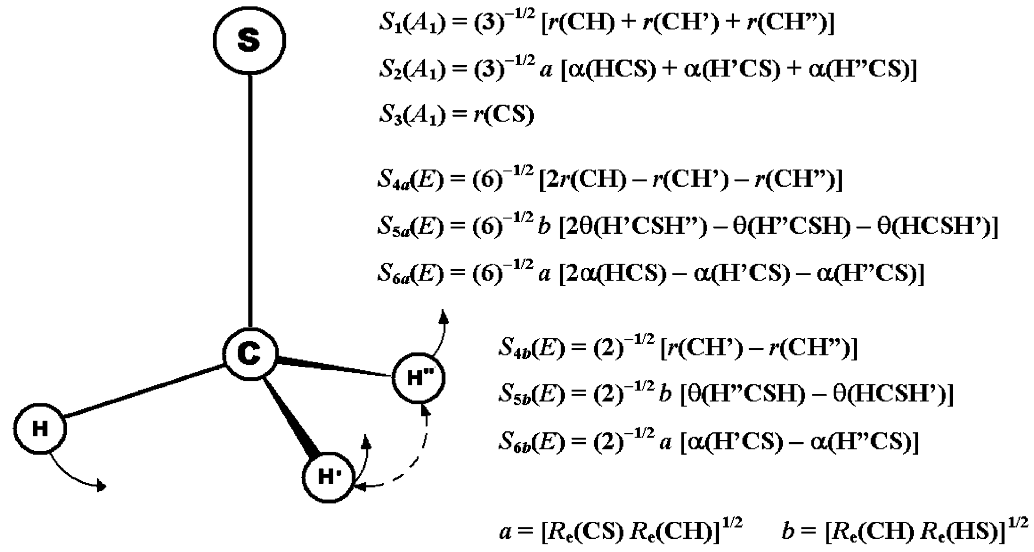

$$S_1(A_1) = (3)^{-1/2}\,[r(\mathrm{CH}) + r(\mathrm{CH'}) + r(\mathrm{CH''})]$$

$$S_2(A_1) = (3)^{-1/2}\,a\,[\alpha(\mathrm{HCS}) + \alpha(\mathrm{H'CS}) + \alpha(\mathrm{H''CS})]$$

$$S_3(A_1) = r(\mathrm{CS})$$

$$S_{4a}(E) = (6)^{-1/2}\,[2r(\mathrm{CH}) - r(\mathrm{CH'}) - r(\mathrm{CH''})]$$

$$S_{5a}(E) = (6)^{-1/2}\,b\,[2\theta(\mathrm{H'CSH''}) - \theta(\mathrm{H''CSH}) - \theta(\mathrm{HCSH'})]$$

$$S_{6a}(E) = (6)^{-1/2}\,a\,[2\alpha(\mathrm{HCS}) - \alpha(\mathrm{H'CS}) - \alpha(\mathrm{H''CS})]$$

$$S_{4b}(E) = (2)^{-1/2}\,[r(\mathrm{CH'}) - r(\mathrm{CH''})]$$

$$S_{5b}(E) = (2)^{-1/2}\,b\,[\theta(\mathrm{H''CSH}) - \theta(\mathrm{HCSH'})]$$

$$S_{6b}(E) = (2)^{-1/2}\,a\,[\alpha(\mathrm{H'CS}) - \alpha(\mathrm{H''CS})]$$

$$a = [R_e(\mathrm{CS})\,R_e(\mathrm{CH})]^{1/2} \qquad b = [R_e(\mathrm{CH})\,R_e(\mathrm{HS})]^{1/2}$$

Figure 1. The C_{3v} nuclear configuration of CH_3S and symmetric vibrational coordinates S. The values of r, α, and θ are internal vibrational coordinates defined as displacements of relevant coordinates from their optimal (equilibrium) values in the C_{3v} nuclear configuration. The dotted and solid curve lines corresponding to S_5 and S_6, respectively, show directions of possible Jahn–Teller distortions in CH_3S.

The constants D and K are dimensionless. The values of E_{JT} and D calculated for any of the Jahn–Teller active modes cannot be negative because $U(C_s, \mathrm{A'}) \leq U(C_{3v}, \mathrm{E})$ whereas Δ_{JT} and g may be negative in the case of $U(C_s, \mathrm{A''}) < U(C_s, \mathrm{A'})$ when the PES minimum corresponds to the A″ electron wave function. It is always true that $0 \leq K \leq 1$. The sign of k depends on the choice of the **L** matrix in eq 1 (**L** and −**L** correspond to the same set of harmonic frequencies). In our calculations, we used $k \leq 0$.

In the absence of quadratic Jahn–Teller coupling ($K = g = 0$), we can evaluate the vibronic levels $E(v, l)$ of a molecule by means of second-order perturbation theory in the single mode approximation[3]

$$E(v,l) = \omega(v + 1) \mp 2E_{\mathrm{JT}}(l \pm 1) \tag{7}$$

where the integer v is a vibrational quantum number of a two-dimensional isotropic harmonic oscillator and l ($l = -v, -v + 2, ..., v - 2, v$) is a vibrational angular momentum quantum number. Assignments of vibronic levels $E(v, l)$ can be made with use of a Jahn–Teller quantum number $j = l \pm {}^1/_2$. As shown in ref 3, eq 7 is valid only for low energy levels with small Jahn–Teller coupling ($D \leq 0.05$).

Energy levels obtained by eq 7 are 2-fold degenerate (with symmetries e or $\mathrm{a_1 + a_2}$). Being accidental, the $\mathrm{a_1 + a_2}$ degeneracy can be eliminated by the quadratic Jahn–Teller coupling. With spin–orbit coupling, the vibronic states are split as $\mathrm{a_1 + a_2 \rightarrow 2e_{1/2}}$, $\mathrm{e \rightarrow e_{1/2} + e_{3/2}}$. The final spin-vibronic levels are transformed according to irreducible representations of the double C_{3v} symmetry group. For the case of a weak linear Jahn–Teller coupling, the spin–orbit splitting ΔE^{SO} of any vibronic level may be approximated for each $j = l \pm {}^1/_2$ as

$$\Delta E^{\mathrm{SO}} = a\zeta_e d \tag{8}$$

$$d = \pm 1 \mp 4E_{\mathrm{JT}}(v + 1)/\omega$$

using a value ($-\,a\zeta_e$) of spin–orbit splitting in the $\mathrm{X^2E}$ ground electronic state at the C_{3v} symmetry nuclear configuration.[3]

In the figures and tables, we use dimensionless a components of the normal coordinates Q_4(E), Q_5(E), and Q_6(E). The relation between q (dimensionless) and Q (in hartree units, Bohr radius × [electron mass]$^{1/2}$) is

$$q = (4.55635 \times 10^{-6} \times \omega\,)^{1/2}\,Q \tag{9}$$

where ω is a relevant unperturbed harmonic frequency (in cm^{-1}).

TABLE 1: The Jahn–Teller Stabilization Energy (E_{JT}, cm^{-1}) and Barrier (Δ_{JT}, cm^{-1}) to Internal Vibronic Pseudorotation in $\mathrm{X^2E}$ CH_3S Calculated at Different Levels of Theory[a]

	$E_{\mathrm{JT}} = U(C_{3v}) - U(C_s, \mathrm{A'})$		$\Delta_{\mathrm{JT}} = U(C_s, \mathrm{A''}) - U(C_s, \mathrm{A'})$	
method	pvtz	pvqz	pvtz	pvqz
CASSCF	41.5	43.2	5.5	5.9
CASSCF (rel)	41.1	42.1	5.4	5.7
PT2	87.6	89.2	15.3	15.2
PT2 (rel)	87.3	87.8	15.2	15.8
CASSCF[b]	53.5		7.7	
SOCI[b]	81.5		13.3	
CASSCF[c]	56.6		9.2	
PT2[c]	92.4		15.8	
EOMIP	91.5	93.2	14.8	14.9

[a] Methods: the complete active space self-consistent field (CASSCF), the multiconfiguration quasi-degenerate second-order perturbation theory (PT2) based on a CASSCF reference wave function, the second-order (with all singles and doubles) configuration interaction method (SOCI) also with a CAS reference, and the equation-of-motion coupled cluster (EOMIP) approach with the CH_3S^--anion CCSD reference state. Calculations of total energies were carried out at geometric parameters optimized by EOMIP/pvqz. The complete active space contains five electrons in four orbitals ($\mathrm{2a_1 + e}$) unless noted otherwise. The notation "rel" designates the calculations involving spin-free relativistic effects. [b] The complete active space contains 13 electrons in 8 orbitals ($\mathrm{4a_1 + 2e}$). [c] The complete active space contains 13 electrons in 11 orbitals ($\mathrm{5a_1 + 3e}$).

Results and Discussion

Calculations without Spin–Orbit Coupling. The Jahn–Teller stabilization energy (E_{JT}) and the barrier to pseudorotation (Δ_{JT}) in the CH_3S $\mathrm{X^2E}$ ground-state calculated at different levels of theory are shown in Table 1.

TABLE 2: The Structural Parameters of the CH_3S Radical[a]

				EOMIP	
C_{3v}(E) parameter	PT2	EOMIP	C_s Parameter	A′, min	A″, max
R_e(CS)	1.8202	1.7940	R_e(CS)	1.7913	1.7919
R_e(CH)	1.0847	1.0872	R_e(CH)	1.0914	1.0843
α_e(HCS)	109.17	109.80	α_e(HCS)	106.38	112.44
θ(HCSH′)	120	120	R_e(CH′)	1.0855	1.0889
$E + 437.0$	−1.664174	−0.591697	β_e(H′CS)	111.45	108.45
E_{JT}	87.8	93.2	θ_e(HCSH′)	117.69	122.01
Δ_{JT}	15.8	14.9	ω_1(A′)	3145(11)	3183(10)
ω_1(A_1)	3072	3066(8)	ω_2(A′)	3057(4)	3062(6)
ω_2(A_1)	1316	1367(3)	ω_3(A′)	1498(10)	1477(8)
ω_3(A_1)	700	758(0.1)	ω_4(A′)	1361(3)	1359(2)
ω_4(E)	3200	3164	ω_5(A′)	886(2)	990(8)
ω_5(E)	1477	1483	ω_6(A′)	750(0.5)	756(0.5)
ω_6(E)	917	938	ω_7(A″)	3170(60)	3115(71)
			ω_8(A″)	1407(100)	1446(100)
			ω_9(A″)	606(84)	595*i*

[a] Values and dimensions: distances *R* (Å), valence angles α, β, and torsions θ (deg), total energies *E* (hartree), Jahn−Teller stabilization energies $E_{JT} = U(C_{3v}, \text{E}) - U(C_s, \text{A}')$ and barriers $\Delta_{JT} = U(C_s, \text{A}'') - U(C_s, \text{A}')$ (cm^{-1}), harmonic frequencies ω_i (cm^{-1}), and infrared intensities (in parentheses, km/mol). The potential energy minimum (min) and the saddle point (max) on PES of the JT-distorted CH_3S radical correspond to $^2A'$- and $^2A''$-electronic states of C_s symmetry, respectively. The unperturbed harmonic frequencies ω_i(E) were calculated by eq 2 (see the text). Calculations of PT2 Jahn−Teller energies were carried out at geometric parameters optimized by EOMIP/pvqz.

The values of E_{JT} and Δ_{JT} calculated by multiconfiguration quasi-degenerate second-order perturbation PT2 theory are similar to those obtained by the equation-of-motion EOMIP method; the differences do not exceed 4 cm^{-1}. The computationally inexpensive PT2 approach yields very reliable results even with an active space as small as “five electrons in four orbitals ($2a_1$ + e)” and with correlation of all doubly occupied noncore orbitals.

The CASSCF approach gives too low values of E_{JT} and Δ_{JT} in comparison with the PT2 and EOMIP results. More extended complete active spaces do not reduce this discrepancy significantly (see E_{JT} (CASSCF) from Table 1, cm^{-1}, 41.5 → 53.5 → 56.6) but cost much more computational time. Apparently, the main reason for this inaccuracy is omission of the dynamical electron correlation in the CASSCF calculations. The very computationally expensive SOCI method (multireference configuration interactions with all doubles and singles) improves the CASSCF results, but the difference between the values of E_{JT} and Δ_{JT} calculated by PT2 (or EOMIP) and those obtained by SOCI still remains relatively large (3−10 cm^{-1}). Our computational experiments suggest that further (hypothetical) extension of a CAS reference in SOCI computations may reduce this disagreement. However, the low computational cost of calculations by PT2 and EOMIP in comparison with SOCI encourages us to prefer the former ones; the time gain with PT2/pvtz and EOMIP/pvtz versus SOCI/pvtz was found to be 1:300.

The basis set extension from triple- to quadruple-ζ quality does not play any significant role in Jahn−Teller energy calculations. Hence, further extension of the basis set would improve our results only a little. Inclusion of scalar relativistic effects (CASSCF (rel) and PT2 (rel) in Table 1) is not critically important. However, we still included these effects for PT2 and SOCPT2 (next section) because it was a no-cost routine. We used the pvqz basis set in all PT2 and EOMIP calculations, results of which are shown below.

The optimized geometries and relevant sets of harmonic frequencies calculated at the C_{3v}(E) symmetry nuclear configuration and in Jahn−Teller distorted structures (A′ and A″) of C_s symmetry are shown in Table 2. The Jahn−Teller energies (E_{JT} and Δ_{JT}) calculated by PT2 and EOMIP are in good coincidence, whereas there is some disagreement in R_e (0.006 Å) and in α_e (0.6°). The inconsistency of harmonic frequencies in PT2 and EOMIP calculations varies from 6 to 58 cm^{-1}. We prefer EOMIP as a more sophisticated approach rather than PT2.

The C_{3v}(E) symmetry geometry calculated here is in good agreement with experimental estimates from ref 7 ($R(\text{C−S}) = 1.791$ Å, $R(\text{C−H}) = 1.090$ Å, $\angle\text{HCS} = 110°$) and in poorer agreement with $R(\text{C−S}) = 1.767 \pm 0.012$ Å, $R(\text{C−H}) = 1.10 \pm 0.02$ Å, $\angle\text{HCS} = 115.8°$ from refs 9 and 16. In general, the calculated equilibrium geometry parameters (r_e) are slightly different from the relevant r_g or r_a values obtained from experimental data.[7,9]

Fragments of potential surfaces of CH_3S calculated by EOMIP without accounting for spin−orbit coupling are shown in Figure 2. The harmonic analysis of specific points on the CH_3S potential energy surfaces was performed (Table 2). The normal modes Q_i in CH_3S (C_{3v}) were assigned to symmetric CH_3 stretching (ω_1), symmetric CH_3 deformation (ω_2, “umbrella”), CS stretching (ω_3), asymmetric CH_3 stretching (ω_4), asymmetric HCH and HCS deformations (ω_5 and ω_6), respectively. The infrared intensities along Jahn−Teller active vibrational modes increase significantly when the molecule is distorted. Comparison of geometries optimized in the C_{3v}(E) symmetry nuclear configuration and in the Jahn−Teller distorted structures (Table 2, Figure 1) shows that in the minimum area (A′) the angle α_e(HCS) is slightly compressed (3.5°) from its nearly tetrahedral value in the unperturbed C_{3v}(E) structure, and therefore α_e(HCS) has to be expanded in the saddle point area (A″). The calculated Jahn−Teller distortions in CH_3S are less appreciable than those in CH_3O.[4,16]

Table 3 contains evaluations of single mode Jahn−Teller energies, vibronic constants, and positions of a minimum and a maximum in the projections of adiabatic surfaces on a single mode Q_{ia} ($Q_{ja} = 0$, $j \neq i$). The Jahn−Teller effect is predicted to be large for HCS bending (Q_6), moderate for HCH deformation (Q_5), and weak for CH_3 stretching (Q_4), compare (in cm^{-1}) $E_{JTi} = 82 \rightarrow 9 \rightarrow 1$. Unlike the Q_4 and Q_6 modes, the relative energies of A′ and A″ electronic states are inverted and the values of Δ_{JT5} and g_{55} become negative.

We calculated the vibronic energy levels of CH_3S by eq 7, taking account of linear Jahn−Teller coupling only in the single mode approximation (Table 4). One can see the splitting of the unperturbed (harmonic oscillator) levels that is largest for the HCS bending (Q_6) mode and less noticeable in the case of Q_4.

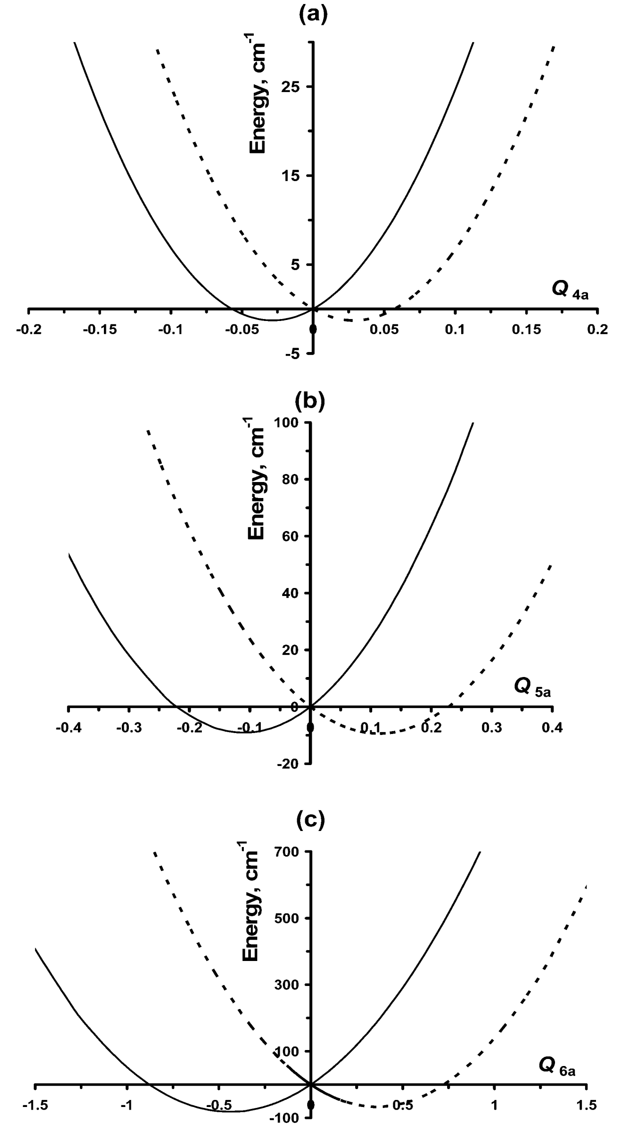

Figure 2. Fragments of potential surfaces of CH_3S calculated by EOMIP without account for spin−orbit coupling, $^2E \rightarrow {}^2A'$ (solid) and $^2A''$ (dotted). The a components of normal coordinates Q_4, Q_5, and Q_6 are dimensionless. The C_{3v} configuration energy is zero.

TABLE 3: The Vibronic Constants Calculated with EOMIP/pvqz and Net Jahn−Teller Effects in CH_3S[a]

	Jahn−Teller active mode		
parameter	$i = 4$	$i = 5$	$i = 6$
$Q_{ia}(A')$	−0.0288	−0.1101	−0.4401
E_{JTi}	1.30	9.08	81.70
$Q_{ia}(A'')$	0.0288	0.1134	0.3617
Δ_{JTi}	0.0002	−0.32	14.81
ω_i	3164	1483	938
$-k_i$	90	166	372
D_i	4.08×10^{-4}	6.24×10^{-3}	7.84×10^{-2}
K_i	7.74×10^{-5}	-1.62×10^{-2}	9.96×10^{-2}
g_{ii}	0.25	−24	93

[a] Values and dimensions: Q_{ia}, D_i, and K_i (dimensionless); E_{JTi}, Δ_{JTi}, ω_i, k_i, and g_{ii}(cm^{-1}). Relations between vibrational constants ω_i, linear (k_i, D_i) and quadratic (K_i, g_{ii}) vibronic constants, and relative energies $E_{JTi} = U_i(C_{3v}, E) - U_i(C_s, A')$, $\Delta_{JTi} = U(C_s, A'') - U_i(C_s, A')$ (see eqs 3−6). Mass-weighted normal coordinates Q_4, Q_5, and Q_6 may be turned into the hartree system units (Bohr radius × [electron mass]$^{1/2}$) by division into a factor of 0.1201, 0.0822, and 0.0654, respectively.

Because the barriers Δ_{JTi} to pseudorotation for Q_4 and Q_5 are very small and $Q_{ia}(A') \approx Q_{ia}(A'') = \rho$ (where ρ is a pseudorotation radius), the linear Jahn−Teller coupling model (so-called Mexican hat, eq 7) may be a good approximation to describe librations governed by these modes.[29] The formula of second-order perturbation theory (eq 7) may be less appropriate for the Q_6 mode where the maximum quadratic Jahn−Teller coupling was predicted.

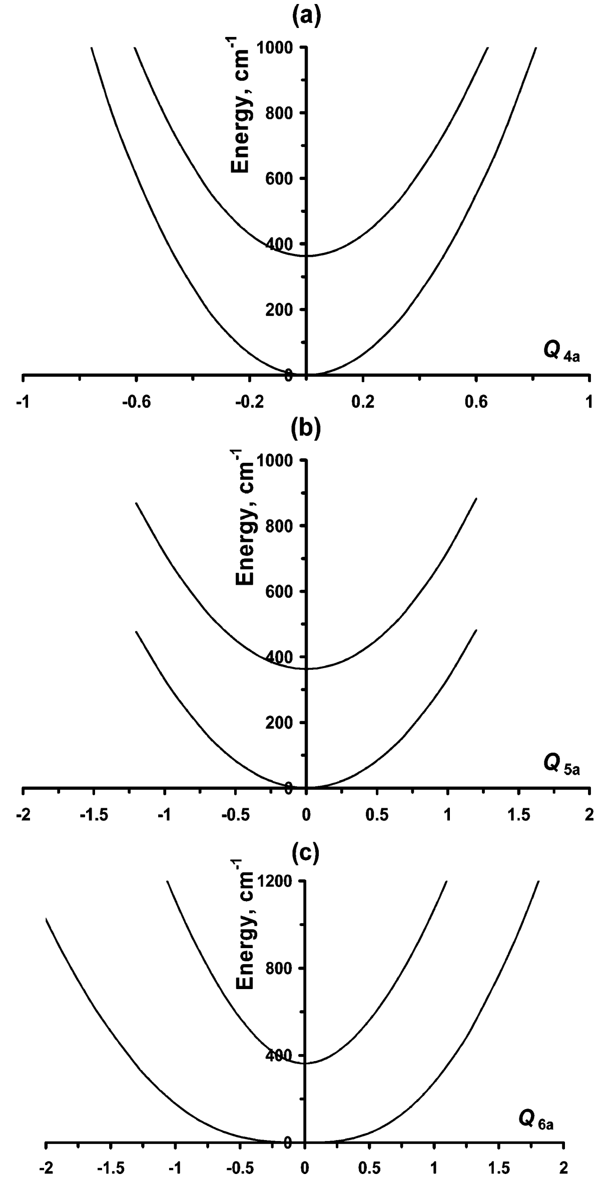

Figure 3. Fragments of potential surfaces of CH_3S calculated by SOCPT2 including spin−orbit coupling. The upper sublevel is $^2E_{1/2}$; the lower one is $^2E_{3/2}$. The a components of normal coordinates Q_4, Q_5, and Q_6 are dimensionless.

Calculations with Spin−Orbit Coupling. The value of spin−orbit splitting in CH_3S X^2E ($-a\zeta_e = 358$ cm^{-1}) was found from SOCPT2/pvqz calculations. Fragments of potential surfaces of CH_3S calculated by SOCPT2 are shown in Figure 3.

The value of $-a\zeta_e$ in CH_3S is significantly larger than the Jahn−Teller stabilization energy along any of the E modes (E_{JT4}, E_{JT5}, E_{JT6} from Table 3). According to a relation obtained in ref 3 between the linear Jahn−Teller effect along a single normal mode (E_{JTi}) and the value of spin−orbit splitting ($-a\zeta_e$), the Jahn−Teller distortions are expected to vanish because of $-a\zeta_e \geq 4E_{JTi}$.[3] In general, the conclusion based on this relation may not be applied for a case with the multimode Jahn−Teller coupling. However, the full SOCPT2 optimization of the geometry parameters of CH_3S followed by a calculation of

TABLE 4: The Vibronic and Spin-Vibronic Energy Levels (cm^{-1}) of CH_3S Evaluated by Second-Order Vibronic Perturbation Theory (without Quadratic JT-Coupling), Their Assignments and Symmetries[a]

		mode 4 (E)		mode 5 (E)		mode 6 (E)					
v	l	E_v	E_{ev}	E_v	E_{ev}	E_v	E_{ev}	E_{sev}	$j = l \pm {}^1/_2$	Γ_{ev}	Γ_{sev}
2	±2	9492	9495	4449	4467	2814	2977	2985	$\pm{}^3/_2$	$a_1 + a_2$	$e_{1/2}$
								2969			$e_{1/2}$
	0		9489		4431		2651	2659	$\pm{}^1/_2$	e	$e_{1/2}$
								2643			$e_{3/2}$
	±2		9484		4395		2324	2332	$\pm{}^5/_2$	e	$e_{3/2}$
								2316			$e_{1/2}$
1	±1	6328	6328	2966	2966	1876	1876	1930	$\pm{}^1/_2$	e	$e_{3/2}$
								1822			$e_{1/2}$
	±1		6323		2930		1549	1603	$\pm{}^3/_2$	$a_1 + a_2$	$e_{1/2}$
								1495			$e_{1/2}$
0	0	3164	3161	1483	1465	938	775	891	$\pm{}^1/_2$	e	$e_{1/2}$
								658			$e_{3/2}$

[a] Calculations were done with linear JT-constants from Table 3 and $-a\zeta_e = 358$ cm^{-1}; see text for details. Assignments of vibronic levels E_{ev} were made with use of the Jahn–Teller quantum number j that is a combination of a vibrational angular moment quantum number l ($l = -v, -v + 2, ..., v - 2, v$) and a label $\Lambda = \pm 1$ distinguishing two components of an electronic function, v is a vibrational quantum number of a two-dimensional isotropic harmonic oscillator. Symmetry of vibronic (E_{ev}) and spin-vibronic (Γ_{sev}) levels designated by lower case letters complies to the following rules: $E \otimes E = a_1 + a_2 + e$, $E \otimes A_1 = E \otimes A_2 = e$, $E_{1/2} \otimes e = e_{3/2} + e_{1/2}$, and $E_{1/2} \otimes a_1 = E_{1/2} \otimes a_2 = e_{1/2}$, where capital letters designate symmetry of basis electronic (E), vibrational (A_1, A_2, and E), and spin ($E_{1/2}$ in the case of $S = {}^1/_2$) functions.

harmonic frequencies confirms that the Jahn–Teller distortions are totally overpowered by the spin–orbit coupling in CH_3S. The C_{3v} equilibrium geometries are equivalent in the $^2E_{3/2}$ and $^2E_{1/2}$ spin–orbit sublevels and correspond to global minima on the relevant PESs (Figure 3). Hence, the suggestion of Suzuki et al.[8] about the difference of $^2E_{3/2}$ and $^2E_{1/2}$ geometries was not supported by theory.

The reduction of the Jahn–Teller effect by spin–orbit coupling does not mean though that the vibronic effects may be completely neglected.[3] The shape of potential surfaces for the two final spin–orbit states is determined by the relation between the $a\zeta_e$ quantity and the values of E_{JTi} and Δ_{JTi} (Table 3). In the case of a vanishing Jahn–Teller effect (Figure 3, part a), the $^2E_{3/2}$ and $^2E_{1/2}$ curves go in a nearly parallel way with a gap of $-a\zeta_e$ like the case of a totally symmetric mode. If a strong Jahn–Teller coupling occurs (Figure 3, part c), the lower and upper states exhibit significantly different curvatures in the equilibrium point; the lower curve is much flatter. The crude evaluation of spin-vibronic energy levels by eqs 7 and 8 is shown in Table 4. This corresponds to the case when the Jahn–Teller effect occurs only in the HCS bending mode (Q_6) and all nonlinear vibronic couplings are neglected. Each vibronic level undergoes spin–orbit splitting, the value of which varies from 233 to 16 cm^{-1}, being always less than $-a\zeta_e$. The energy difference between the two lowest spin-vibronic sublevels ($-a\zeta_e d = 233$ cm^{-1}) should be interpreted as a spin–orbit splitting of the zero energy vibrational level. The Ham reduction factor d shows how much the spin–orbit coupling $a\zeta_e$ is reduced by the Jahn–Teller effect. The quantity of $a\zeta_e d$ can be observed in the spectrum.

Our evaluations of $E_{JT} = 93$ and $-a\zeta_e = 358$ cm^{-1} are in very good agreement with those obtained by Bent[18] from the spectroscopic data ($E_{JT} = 95$ and $-a\zeta_e = 356$ cm^{-1}). The values of $E_{JT} = 41$ and $-a\zeta_e = 341$ cm^{-1} calculated by Barckholtz and Miller[3] seem to be underestimated. The theoretical value of $-a\zeta_e d = 233$ cm^{-1} is close to the observed ones: 220.3[7] (microwave spectroscopy); 259.1,[2] 280 ± 20,[8] and 255.5[9] (laser-induced fluorescence); 280 ± 50[12] and 265 ± 15[13] (photoelectron spectroscopy). The inaccuracy of our value of $a\zeta_e d$ is mostly defined by numerical errors of spin-vibronic energies calculated by means of second-order perturbation theory (with the omission of nonlinear and multimode vibronic couplings).

Summary

This study presents results of the first accurate calculation of linear, quadratic, and spin-vibronic constants and adiabatic Jahn–Teller surfaces in X^2E CH_3S performed with use of advanced computational methods accounting for dynamical electron correlation (equation-of-motion coupled cluster and multiconfiguration quasi-degenerate second-order perturbation theories) and basis sets of triple- and quadruple-ζ quality. To the best of our knowledge, this is the first ab initio computation of spin–orbit coupling that has been ever done for any of the CX_3Y (CH_3O, CH_3S, CF_3O, and CF_3S) species. Analysis of the literature[3] and results of this study show that all these species exhibit quite different relations of the Jahn–Teller effect to the spin–orbit coupling. The spin–orbit coupling in the sulfur-centered radicals is very large with respect to the Jahn–Teller effect (358 versus 93 cm^{-1} in X^2E CH_3S, this study) and totally overpowers JT distortions in CH_3S and CF_3S. However, the oxides CH_3O and CF_3O are structurally distorted by the Jahn–Teller effect accompanied by a relatively small SOC.

Acknowledgment. Acknowledgements are made to the donors of the ACS Petroleum Research Fund and to the Welch Foundation (Grant F-100) for support of this research. It is also a part of Project No. 2000-013-1-100 of the International Union of Pure and Applied Chemistry (IUPAC) entitled "Selected Free Radicals and Critical Intermediates: Thermodynamic Properties from Theory and Experiment" (inquiries to T. Berces, berces@chemres.hu). We wish to thank John Stanton for use of his expanded version of the ACESII program and for helpful discussions. We appreciate also interesting comments and advice from Isaac Bersuker, Valery Sliznev (ISUCT, Ivanovo, Russia), and Nikolai Balabanov (WSU, Pullman).

References and Notes

(1) Brossard, S. D.; Carrick, P. G.; Chappell, E. L.; Hulegaard, S. C.; Engelking, P. C. *J. Chem. Phys.* **1986**, *84*, 2459.
(2) Chiang, S.-Y.; Lee, Y.-P. *J. Chem. Phys.* **1991**, *95*, 66.
(3) Barckholtz, T. A.; Miller, T. A. *Int. Rev. Phys. Chem.* **1998**, *17*, 435.
(4) Höper, U.; Botschwina, P.; Köppel, H. *J. Chem. Phys.* **2000**, *112*, 4132.
(5) Jacox, M. E. *J. Phys. Chem. Ref. Data* **2003**, *32*, 1.
(6) Ohbayashi, K.; Akimoto, H.; Tanaka, I.*Chem. Phys. Lett.* **1977**, *52*, 47.
(7) Endo, Y.; Saito, S.; Hirota, E. *J. Chem. Phys.* **1986**, *85*, 1770.
(8) Suzuki, M.; Inoue, G.; Akimoto, H. *J. Chem. Phys.* **1984**, *81*, 5405.

(9) Hsu, Y.-C.; Liu, X.; Miller, T. A. *J. Chem. Phys.* **1989**, *90*, 6852.

(10) Anastasi, C.; Broomfield, M.; Nielsen, O. J.; Pagsberg, P. *Chem. Phys. Lett.* **1991**, *182*, 643.

(11) Engelking, P. C.; Ellison, G. B.; Lineberger, W. C. *J. Chem. Phys.* **1978**, *69*, 1826.

(12) Janousek, B. K.; Brauman, J. I. *J. Chem. Phys.* **1980**, *72*, 694.

(13) Schwartz, R. L.; Davico, G. E.; Lineberger, W. C. *J. Electron. Spectrosc. Relat. Phenom.* **2000**, *108*, 163.

(14) Bise, R. T.; Choi, H.; Pedersen, H. B.; Mordaunt, D. H.; Neumark, D. M. *J. Chem. Phys.* **1999**, *110*, 805.

(15) Pushkarsky, M. B.; Applegate, B. E.; Miller, T. A. *J. Chem. Phys.* **2000**, *113*, 9649.

(16) Barckholtz, T. A.; Miller, T. A. *J. Phys. Chem. A* **1999**, *103*, 2321.

(17) Resende, S. M.; Ornellas, F. R. *Chem. Phys. Lett.* **2003**, *367*, 489.

(18) Bent, G. D. *J. Chem. Phys.* **1988**, *89*, 7298.

(19) Stanton, J. F.; Gauss, J.; Watts, J. D.; Lauderdale, W. J.; Bartlett, R. J. *Int. J. Quantum Chem., Quantum Chem. Symp.* **1992**, *26*, 879.

(20) Schmidt, M. W.; Baldridge, K. K.; Boatz, J. A.; Elbert, S. T.; Gordon, M. S.; Jensen, J. H.; Koseki, S.; Matsunaga, N.; Nguyen, K. A.; Su, S. J.; Windus, T. L.; Dupuis, M.; Montgomery, J. A. *J. Comput. Chem.* **1993**, *14*, 1347.

(21) Dunning, T. H., Jr. *J. Chem. Phys.* **1989**, *90*, 1007. Woon, D. E.; Dunning, T. H., Jr. *J. Chem. Phys.* **1993**, *98*, 1358. Basis sets were obtained from the Extensible Computational Chemistry Environment Basis Set Database, Version 12/03/03, as developed and distributed by the Molecular Science Computing Facility, Environmental and Molecular Sciences Laboratory which is part of the Pacific Northwest Laboratory, P.O. Box 999, Richland, WA 99352, USA, and funded by the U.S. Department of Energy. The Pacific Northwest Laboratory is a multi-program laboratory operated by Battelle Memorial Institute for the U.S. Department of Energy under contract DE-AC06-76RLO 1830. Contact David Feller or Karen Schuchardt for further information.

(22) Stanton, J. F.; Gauss, J. *J. Chem. Phys.* **1994**, *101*, 8938.

(23) Granovsky, A. A. http://classic.chem.msu.su/gran/gamess/index.html.

(24) Nakano, H. *J. Chem. Phys.* **1993**, *99*, 7983.

(25) Fedorov, D. G.; Koseki, S.; Schmidt, M. W.; Gordon, M. S. *Int. Rev. Phys. Chem.* **2003**, *22*, 551.

(26) Nakajima, T.; Hirao, K. *Chem. Phys. Lett.* **1999**, *302*, 383.

(27) Sliznev, V. V. Private communication. Solomonik, V. G. Doctor in Chemistry Thesis, Moscow State University, 1993.

(28) Cyvin, S. J. *Molecular Vibrations and Mean Square Amplitudes*; The Norwegian Research Council for Science and the Humanities: Universitetsforlaget, Norway, 1968.

(29) Bersuker, I. B.; Polinger, V. Z. *Vibronic Interactions in Molecules and Crystals*; Springer-Verlag: Berlin, New York, 1989.